

# Artificial Neural Network Modelling to Optimize Micro-Drilling Parameters of ECDM of Developed Novel Zn/(Ag+Fe)-MMC

Inderjeet Singh Sandhu\*

## Abstract

Several engineering fields have increased their use of metal matrix composites (MMCs) in the past few years. Due to the increase in composites, the demand for accurate machining has also become important. Specifically, pertaining to biomaterial applications, accuracy factor with desired surface finish is critical. While the near-net shape manufacturing process has advanced, MMCs frequently require post-mould machining to achieve surface quality, and dimensional tolerances. In the present study, a zinc MMC (ZMMC) is fabricated and its mechanical properties are tested. Taguchi's orthogonal array (L18) is used to determine the machineability of novel Zn/(Ag+Fe)-MMC. As part of the current work, an artificial neural network (ANN) is implemented to model and optimize materials removal rate (MRR), overcut ( $O_c$ ), and tool wear (TW) during electrochemical discharge machining (ECDM) of novel Zn/(Ag+Fe)-MMC. In order to obtain the response/output values, ECDM micro-drilling experiments were conducted under different input control factors such as pulse-on-time, current, pulse-off-time, and feed rate. It identified that 4-16-3-3 was the best architecture for the ANN model. The root mean square error (RMSE) from the optimization model was used to evaluate performance. Based on regression coefficients between experimental and model predictions and the correlation coefficient (R-value) between the ANN predictions and experimental results, the performance of the model was evaluated. The overall R-index was assessed as 0.98722. During the experiment it was found that training, validation and testing results are 98.782%, 98.122% and 98.505%, respectively. ANN modelling and prediction analysis succeeded in replacing conventional method of regression analysis in field of machining hybrid materials.

**Keywords:** Artificial neural network, micro-drilling, optimization, metal matrix composite, electrochemical discharge machining, correlation coefficient, prediction

## INTRODUCTION

Artificial intelligence (AI), specifically artificial neural networks (ANNs), has allowed manufacturing to make revolutionary progress. However, neural networks (NNs) received less attention in the field of AI application in the production industry. Most important features of ANNs

are: (i) self-adaptive behavior improves the network's ability to learn and to predict, allowing it to adapt forecasts to changing ecological conditions; (ii) from speech and natural language processing to imaging and biomedical engineering, parallel computing has a profound impact on many disciplines and applications. Hence, they can be of significant benefit for today's computer integrated smart factories and manufacturing, in the context of Industry 4.0. Manufacturers are making rapid changes in their manufacturing processes due to shifting customer demands and shorter product

### \*Author for Correspondence

Inderjeet Singh Sandhu  
E-mail: sandhuinderjeet248@gmail.com

Research Scholar, Department of Mechanical Engineering,  
Punjab Engineering College, Chandigarh, Punjab, India

Received Date: December 21, 2022  
Accepted Date: March 19, 2023  
Published Date: June 19, 2023

**Citation:** Inderjeet Singh Sandhu. Artificial Neural Network Modelling to Optimize Micro-Drilling Parameters of ECDM of Developed Novel Zn/(Ag+Fe)-MMC. Journal of Polymer & Composites. 2023; 11(Special Issue 1): S1-S13.

lifetimes. To adapt to these changes, manufacturing technologies must be versatile. The solution to this problem can be achieved by using artificial neural networks. There are a wide variety of applications of ANN, including classification, forecasting, modelling, optimization, and recognition etc. These applications are relevant to a wide range of real-life problems in sectors including aviation, automotive, defense, engineering, and medical [1, 2]. Simulating the structures and functions of biological neural networks and neurons, ANNs are basic models of the human central nervous system [3]. ANNs by their nature do not work serially but work more like a parallel mode, where each component of the network performs a separate function and is dispersed throughout all of the neurons [4].

Thus, ANNs work in a similar manner to enormous parallel dispersed processors, which consist of simple processing neurons and increase the number of computing resources available [5]. Many researchers around the world are conducting ongoing research into manufacturing processes, such as drilling, milling, turning, laser cutting, electrochemical discharge machining (EDM), and plasma arc cutting, etc. [6, 7]. Soft computation methods are applied to model and quality objectives were optimized, such as dimensional accuracy, delamination factors, materials removal rate (MRR), and residual stress and surface roughness characteristics, for example [8–11]. A high degree of complexity and uncertainty characterizes the laser cutting (LC) process due to the complex thermomechanical and physical processes developed during the machining process [12, 13]. In other words, conventional models that are based on machining theory and analytical models to estimate LC quality characteristics work perfectly for a specific set of processes, defined conditions, and specific technologies [14]. Machine learning (ML) techniques like ANN, genetic algorithm and fuzzy logic serve as a black box and are unaffected by the process itself, making them an excellent choice for control, modelling, monitoring, and optimization of such applications [15–18]. McDonnell et al. [16] used ANN with three identical blocks for parameters optimization for wear control applications, followed by two full-connected layers and a finally, single activation layer. A  $1 \times 10^{-5}$  learning rate was chosen, lower than average. The study concluded that the proposed approach to laser process optimization can be used in a widespread series of fields and help to cut the cost and time associated with it. Design phase comprises a number of factors that affect its performance are included. The factors can be grouped into six general categories, based on Madic and Radovanović [19]: dataset for the ANN, iterations' number, type of transfer function, initialization of weight (variable weights or equal as per requirement), training algorithm, and ANN's architecture. Undoubtedly, a systematic approach has not been found to select the optimal training parameters of an ANN. In most cases, the process involves trial-and-error experiments, which require knowledge and time of each participant [12]. Through literature review, number of hidden layers are determined. Then proceeding with a simulation of ANNs of various sizes (3, 4, 5, . . . , N) follows, with the aim of obtaining the least mean squared error (MSE) and root MSE (RMSE) performance [12].

Modelling by using these methods does not always lead to the desired results. In addition, according to the literature, most research on optimization of neural networks focuses on optimizing only the MSE and RMSE. As well, optimizing only a single objective of an ANN at a time is typically not implemented concurrently with optimizing multiple objectives simultaneously utilizing multi-objective optimization techniques [20]. Additionally, ANN methodology is opted to replace existing regression analysis technique for even small dataset. An attempt is made to use ANN model in mechanical engineering field specially focusing machining studies which are conventionally utilizing regression analysis.

In this study, novel Zn/(Ag+Fe)-MMC is developed using liquid stir casting parameters. Afterwards, fabricated slab underwent micro-drilling under four different input parameter conditions. Three different types of output parameters were extracted. Further, these features were used for multi objective optimization using ANN. As the final step, predictive analysis is performed to measure RMSE and compared with experimental observations. Figure 1 represents methodology used to carry out ANN modelling.

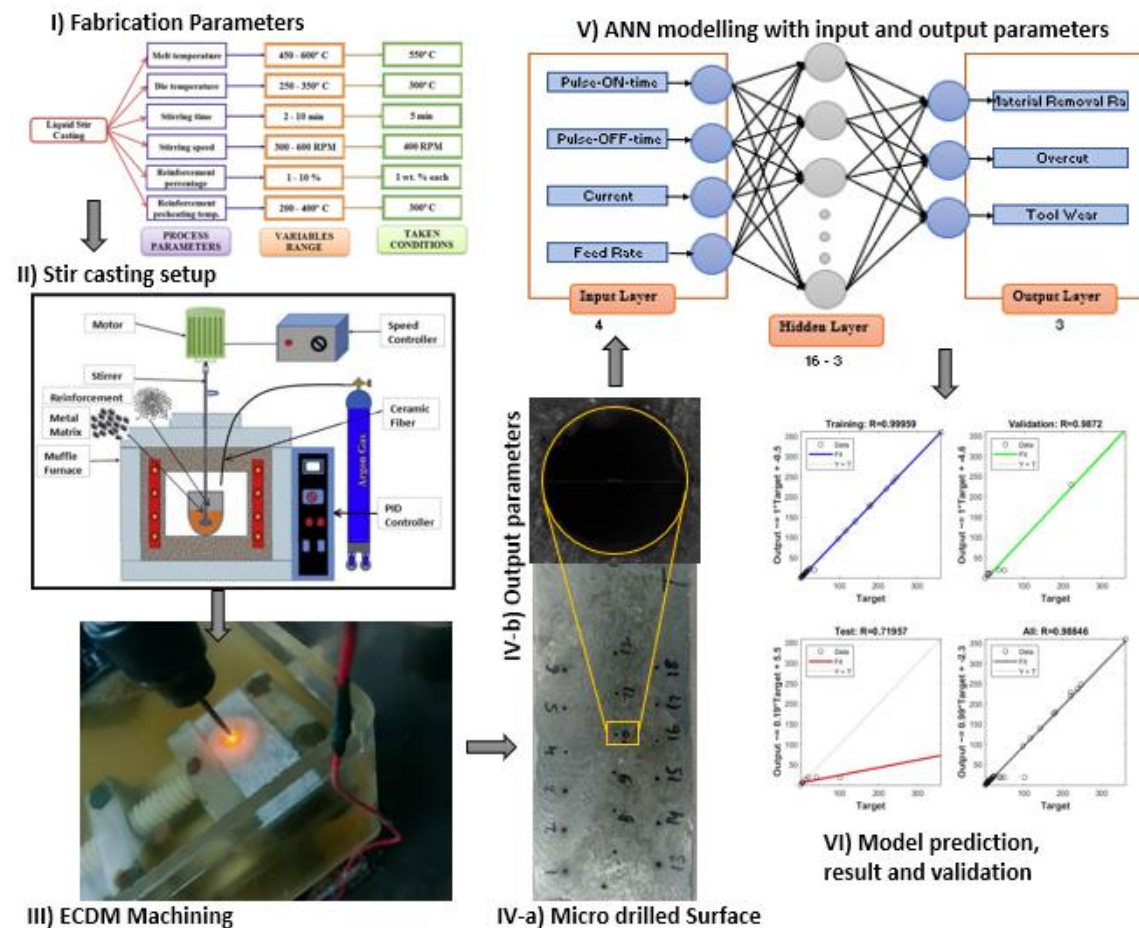


**Figure 1.** Methodology followed to model artificial neural network (ANN) for developing Zn/(Ag + Fe)-metal matrix composite (MMC).

### ECDM PROCESS

Electrical discharge machining is combined with electrochemical machining to form electrochemical discharge machining. ECDM is a process that involves electrochemical reactions and electrical spark discharges (ESDs) to remove material. One of the most significant electrolysis processes is the formation of a gas film. Gas film formation is key because sparks/discharges occur within the film, which ultimately improves machining performance. As bubbles coalesce to form larger bubbles as current density increases, an electric field is detected at the wire electrode surface. A high enough potential difference can break the electric field during electrochemical reactions, causing sparks to be generated. Electrical discharges result in discontinuous sparking, subsequently removing material from the workpiece. A spark that results in an electrical charge striking the work material raises the material's temperature to its melting point. In addition to promoting chemical reactions, high temperatures also boost electrolyte reactions. ECDM removed material from the workpiece by melting, vaporizing, and chemically action.

### Experimental Details of Micro-Drilled Surface of Novel Zn/(Ag+Fe)-MMC Using ECDM Setup Details of Work Piece

The zinc metal matrix composite (ZMMC) was fabricated utilizing liquid stir casting. Nanoparticles were reinforced after being pre-heated. Figure 2 represents different views of fabricated MMC.

An investigation developed in this area focuses on ZMMCs reinforced with 1 wt% of silver and 1 wt% of iron nanoparticles. A sample with a width of 32 mm, a length of 80 mm, and having a thickness of 6 mm is selected for micro-drilling using ECDM setup as shown in Figure 3. In recent

years, zinc alloys have gained a lot of attention. They are used in automobile, biomedical, electronic, pharmaceutical, medical, and marine applications due to their low friction, light weight, and corrosion resistance [21]. Consequently, ZMMCs need to be investigated.



**Figure 2.** After fabrication, top and side view of metal matrix composite (MMC).

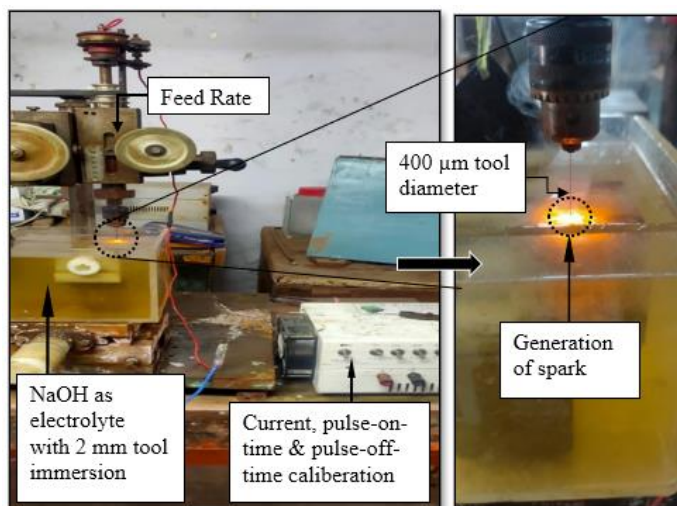


**Figure 3.** Experimental setup of electrochemical discharge machining (ECDM).

### ***Microstructure Analysis***

Optical microscopy was used for microstructure at 200× magnification as shown in Figure 4(a). Uniform distribution of particles is clearly visible with some cluster formations. Accumulation of Fe particles around Ag particles can be seen. Clear zinc dendritic formations are visible throughout the matrix. Into dendritic zones, Fe particles are visible as confirmed by scanning electron microscopy (SEM) as shown in Figure 4(b). SEM is performed at scale of 100 μm magnification. Base material (zinc) is present in area having dark gray shades, while black shade is due to Ag nanoparticles. Fe particles are present in vicinity of Ag particles depicting whitish shade. Energy dispersive spectroscopy (EDS) mapping is also provided as shown in Figure 4(c) at 100 μm magnification.

### ***Experimental Setup and Constructing Taguchi Orthogonal Array***

This study used Taguchi's orthogonal array (L18) to determine the machineability of novel Zn/(Ag+Fe)-MMC. Analyses and optimizations were performed with MATLAB. In order to micro-drill with a brass cutting tool of 400 μm in diameter with the selected process parameters, four parameters, namely, pulse-on-time ( $T_{on}$ ), pulse-off-time ( $T_{off}$ ), feed rate (FR), and current (C) were selected. Calculated output responses were material removal rate (MRR), overcut ( $O_c$ ), and tool wear (TW). Three levels of  $T_{on}$ , FR, and C were varied, while two levels of  $T_{off}$  were varied. Drilling trials were conducted in 18 experiments using a mixed level orthogonal level approach. Table 2 shows the input variable parameters like pulse-on-time, pulse-off-time, feed rate, and current, as well as their corresponding levels, while Table 3 presents the output responses for each run.

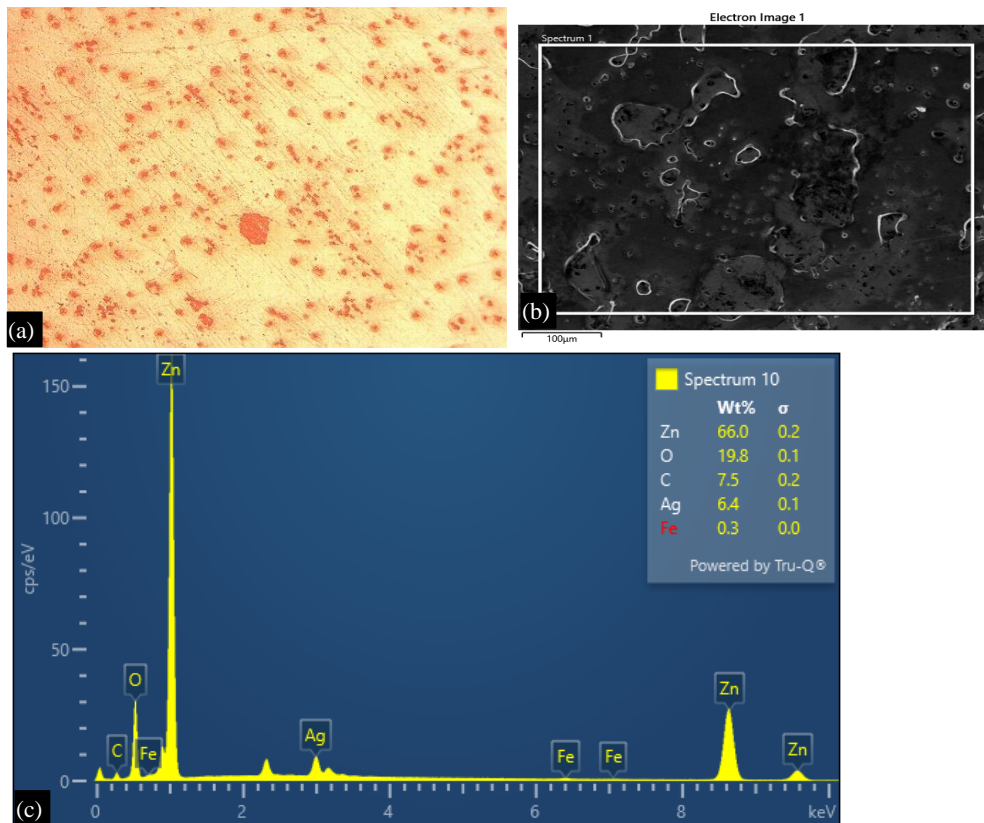


**Figure 4.** (a) Optical images of microstructure at 200 $\times$  magnification using optical microscopy. (b) Scanning electron micrograph of 100  $\mu\text{m}$  magnification. (c) The corresponding energy dispersive spectroscopy (EDS) mapping of the metal matrix composite (MMC) at 100  $\mu\text{m}$  magnification.

As shown in Table 1, L18 array runs correspond to micro-drilled surfaces obtained after machining on ECDCM setup as shown in Figure 3. These images represent the top and bottom machined surfaces of each slab. The top and bottom surfaces of experiments 13 and 14 are depicted in Table 1, along with drilled views of those experiments.

**Table 1.** Micro-Drilled surfaces of metal matrix composite (MMC) (top and bottom surface).

S.N.	Top Drilled Surface	Bottom Drilled Surface
General view		
1		
2		

**Table 2.** Input variable parameters with corresponding levels

Parameters	Symbols	Levels		
		1	2	3
Pulse-off-time (ms)	T <sub>off</sub>	1	2	
Current (A)	C	1	2	3
Pulse-on-time (ms)	T <sub>on</sub>	1	2	3
Feed rate (mm/min)	FR	100	250	500

MRR (mm<sup>3</sup>/min) is calculated as the difference between the weight of the workpiece before and after drilling, as shown in Equation (1). TW (mg) is assessed by comparing the weight of the tool before and after each  $\mu$ -drill as shown in Equation (2). Using Equation (3), O<sub>c</sub> ( $\mu$ m) is calculated by taking the difference between the tool and drilled diameters.

$$MRR = \frac{\pi T}{12 t} \left[ \frac{D_t^3 - D_b^3}{D_b} \right] \times 1000; \quad (1)$$

$$O_c = D_{tool} - \left( \frac{Dt + Db}{2} \right); \quad (2)$$

$$TW = W_i - W_f \quad (3)$$

Above equations tells us that W<sub>i</sub> is the initial weight, W<sub>f</sub> is the final weight, t is the machining time in minutes, T is thickness of fabricated novel ZMMC and  $\rho$  is the density of the material. D<sub>tool</sub> is tool diameter, while, Dt and Db are top and bottom machined diameters, respectively (Tables 2 and 3).

**Table 3.** Experimental results of micro-drilling

Input Values				Output Values		
Ton	Current	Toff	FR	MRR	O <sub>c</sub>	TW
1	1	1	100	21.1608	3.81	<b>0.0072</b>
1	1	2	250	96.9876	8.3835	0.009
1	1	3	500	246.8772	13.9255	0.0145
1	2	1	250	116.298	<b>2.3855</b>	0.0152
1	2	2	500	220.4256	8.3205	0.0249
1	2	3	100	49.3572	12.7985	0.0391
1	3	1	500	<b>361.4988</b>	5.885	0.0257
1	3	2	250	40.5582	5.2875	0.017
2	3	3	100	35.268	6.5535	0.0177
2	1	1	100	22.9242	6.9655	0.0112
2	1	2	250	141.0726	13.0401	0.0137
2	1	3	500	220.4262	17.1075	0.0188
2	2	1	250	180.7494	15.4565	0.0163
2	2	2	500	176.3412	11.4215	0.0227
2	2	3	100	101.3958	12.764	0.0326
2	3	1	500	238.062	3.1295	0.0318
2	3	2	100	19.3974	3.8835	0.0184
2	3	3	250	35.268	9.1235	0.0192

FR, feed rate; MRR, materials removal rate; O<sub>c</sub>, overcut; TW, tool wear.

## ANN MODEL DEVELOPMENT AND IMPLEMENTATION

ANNs were developed by replicating biological learning processes in the brain through learning techniques. With a given sample set, neural networks are robust in predicting a value following a learning activity. To predict the unknown output parameter in various processes, ANNs combine a set of computation procedures with a theoretical basis. Neurons usually consist of a large number of

simple, parallel processors (units). The processors have small amounts of local memory. A communication channel (connection) is used to link two or more units and to convey data, which is encoded in one of several different ways [22]. Supervised network training is done by multilayer perceptron (MLP) using backpropagation algorithm (BPA). The BPA method is a form of steepest descent, in which weight values are adjusted iteratively while moving on the error surface. This ensures that the network arrives at the least amount of error when patterns are presented to the network during the learning process. A forward and a backward pass are made through the layers of a network in order to learn. Layer by layer, the input pattern propagates through the network by applying it to the nodes of the input layers.

A synaptic weight is fixed for the forward pass. A backward pass is used in order to update the synaptic weights when the error is propagated between the actual and the desired output. When a new pattern of input is presented to the network, the weights are continually updated, and the process continues until the network's actual output approaches the desired output. The network cycle is defined as a group of all input patterns propagated once known as epochs.

The majority of practical applications are based on these networks. A popular neural network is a multilayer perceptron or back-propagation neural network (BPNN). This is one of the many different neural networks that have been developed. BPNN is chosen for this paper as it offers several advantages over the other network and has been successfully applied in a wide variety of applications [23]. Back propagation is the most famous neural network training algorithm. However, many problems benefit from modern second-order algorithms, such as conjugate gradient descent or Levenberg-Marquardt (LM), though back propagation may still have an advantage in some instances. It is also the easiest algorithm to understand. Additionally, there are heuristic modifications to the BPA, such as delta-bar-delta and quick propagation that support some problem domains. A BPNN is composed of four input neurons, corresponding to pulse-on-time, pulse-off-time, feed rate, and current, as well as three output neurons, which are corresponding to material removal rate, overcut, and tool wear. A total of one hidden layer has been used with 16 neurons. Input values were normalized before training. Figure 5 shows the ANN configuration.

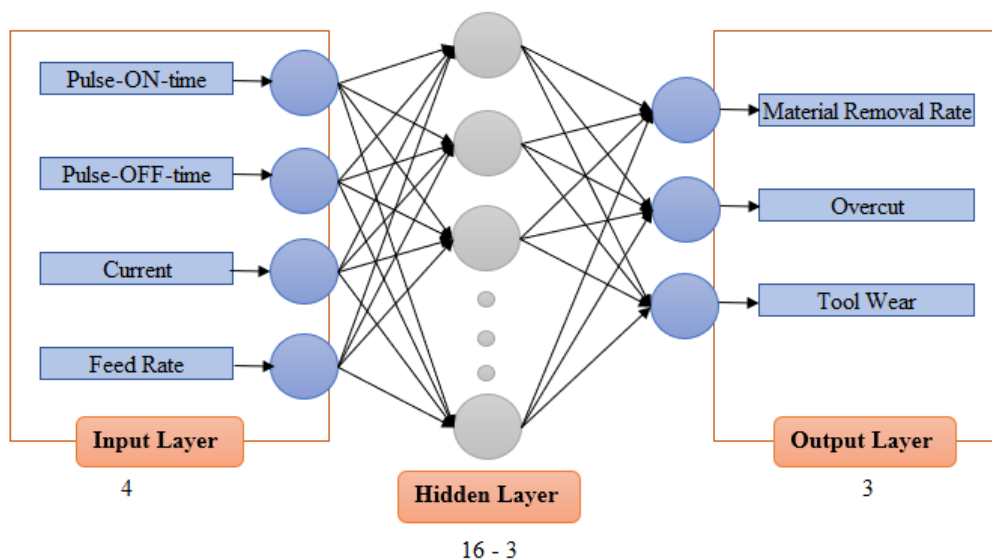


**Figure 5.** Artificial neural network layers depicting 4–16–3–3 configurations.

### Neural Network Algorithm and Architecture

The hidden layer of the ANN contains a variable number of neurons. A total of 16 neurons are present in the hidden layer. Due to a reduced error value, 16 hidden neurons and one hidden layer are used in this configuration. For predicting the material removal rate, overcut, and tool wear, we chose a

neural network model with a 4-16-3-3 topology, as shown in Table 4. Figure 6. illustrates the schematic view of the developed optimized ANN architecture.

**Table 4.** Critical observations for output response model.

S.N.	Inputs	Remarks
1	Network configuration	4-16-3-3
2	Number of input parameters	4
3	Number of output parameters	3
4	Number of hidden layers	1
5	Number of hidden neurons	16
6	Number of output neurons	3
7	Input training function	TrainR (Random weight/bias rule)
8	Adaption learning function	LearnGDM
9	Transfer function used	Logsig (sigmoid)
10	Error calculating method	MSE (mean squared error)
11	Number of epochs	1500

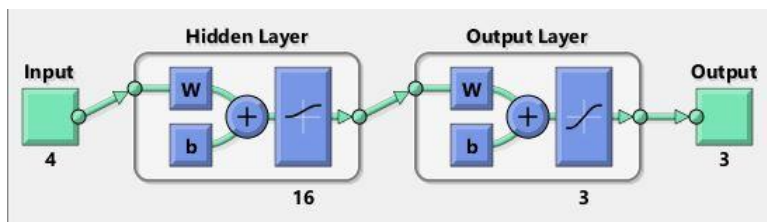


**Figure 6.** Optimum neural network configuration for modelling.

*Step 1:* The number of layers hidden should be determined.

*Step 2:* Identify the number of neurons that each layer will contain. There are as many neurons in the input layer as there are input variables, and similarly, count for the output layers. Set few neurons in the hidden layer.

*Step 3:* Input training pattern is determined.

*Step 4:* Input, hidden, and output layers are assigned with small weight values and below Figure 6. describes optimum NN configuration.

*Step 5* To find the output values (response parameters) for all the neurons in each hidden layer as well as output layer, Equation (4) is used.

$$out_i = s(net_1) = s(\sum w_{ij} out_j + \theta_1) \quad (4)$$

where,  $out_i$  is the  $i$ th output neuron (layer under consideration);  $out_j$  is the  $j$ th output neuron (preceding layer).  $s$  is the sigmoid function, which can be expressed as Equation (5):

$$s(net_1) = \frac{1}{1 + e^{-net_1/q}} \quad (5)$$

where,  $q$  represents the value of temperature.

*Step 6:* The output layer should be determined, then those values should be compared to the desired output. Determining the neuronal error, following Equation (6) is used:

$$error\ obtained = Expected\ Output - Actual\ Output \quad (6)$$



Similarly, RSME value of the output neurons is determined utilizing Equation (7).

$$e_p = \frac{1}{2} \sum (t_{pj} - O_{pj})^2 \quad (7)$$

where,  $e_p$  is  $p$ th presentation vector error,  $t_{pj}$  is the  $j$ th output neuron of expected value and  $O_{pj}$  is the  $j$ th output neuron providing expected output.

*Step 7:* In the hidden layer, calculate the errors associated with each neuron and backpropagate them to the *weight values between those neurons*.

*Step 8:* Calculate from Step 3 through Step 7. The root mean-square error value, and the worst error percentage are determined at the end of the cycle. The next step is to determine if it has a reasonable error. If it does, continue to Step 9. If not, return to Step 3 and repeat the process from Step 3 to Step 7.

*Step 9:* At the end of the iteration, note the final weight values attached to the hidden layer neurons and the output layer neurons.

*Step 10:* Testing the neural network model with the trained weight values, finding the output for the testing pattern and determining whether the deviation from the desired value is reasonable or not. In that case, alter learning rate parameters, change momentum value and change temperature by changing the number of neurons in the revised network. Table 5 shows typical network performance parameters when the configuration is tested.

## RESULTS ANALYSIS AND ANN MODELLING FOR ECDM MICRO-DRILLED PARAMETERS

Simulating the machining parameters of the ECDM in order to establish an association with the performance parameters was the objective of this study. To develop the ANN model, MRR,  $O_c$ , and TW were considered the output variables, whereas the parameters of the process were considered the inputs. Toolbox of MATLAB 2017 was used to implement the ANNs. More than 1000 different network architectures were investigated and analyzed using a "trial-and-error approach".

**Table 5.** Artificial neural network (ANN) model predictive results

Runs	Predicted Value			RMSE Value		
	MRR	$O_c$	TW	MRR	$O_c$	TW
1	20.8557	3.7234	0.011064	0.071915	0.020417	0.000911
2	96.4237	8.3671	<b>0.0077121</b>	0.13292	0.003874	0.000304
3	248.2926	13.9671	0.0136295	0.333613	0.009813	0.000205
4	116.2034	<b>2.6489</b>	0.0123869	0.022287	0.062077	0.000663
5	229.4814	8.5512	0.0191047	2.134473	0.054384	0.001366
6	19.3974	12.3156	0.039745	7.061593	0.113828	0.000152
7	<b>360.3469</b>	5.8688	0.0277876	0.271505	0.003814	0.000492
8	19.4026	6.5273	0.018254	4.986423	0.292224	0.001474
9	19.3974	7.7483	0.018953	3.740736	1.224426	0.001474
10	23.2361	6.9747	0.013637	0.073523	0.002167	0.000574
11	139.9898	13.0084	0.010878	0.255218	0.007469	0.000665
12	220.0402	16.7842	0.0187501	0.090981	0.076212	0.002369
13	179.898	15.5935	0.018866	0.200682	0.032294	0.001752
14	176.5261	11.4269	0.0183644	0.043586	<b>0.001268</b>	0.003379
15	19.3975	12.99	0.034328	19.32718	0.053259	0.000407
16	237.7162	3.1632	0.02796	0.081496	0.007954	0.005619
17	19.3974	5.1199	0.0191	<b>6.06E-06</b>	0.527125	<b>0.000165</b>
18	19.4011	9.1333	0.020296	3.739864	0.002302	0.001437

MRR, materials removal rate; Oc, overcut; RMST, root mean squared error; TW, tool wear.

The study evaluated the ANN simulation model's ability to predict machining properties by comparing the input data with experimental findings. When machining, ANN can be used to predict the maximum material removal rate, while keeping the amount of overcut and tool wear to a minimum. Analyzing the training data and testing values has been done, and graphs have been plotted.

The results of this analysis are summarized in Table 5, which revealed that the values derived from the ANN simulation were more reliable than those derived from the manual process. Training set of fraction values resulted in good modelling of ANN, hence predicting accurate results with minimal error. Consequently, the neural network has demonstrated significant accuracy in predicting the machining properties of ECDM, under a specific set of micro-drilling conditions.

The performance of the ANN model was evaluated by comparing prediction and observed values using the R-value. During the training phase, validation phase, and testing phase, the data presented to the ANN estimates the regression index (R) value that constructs the correlation between the output and the target data. The outcomes are highly correlated with the target data using regression plots as shown in Figure 7.

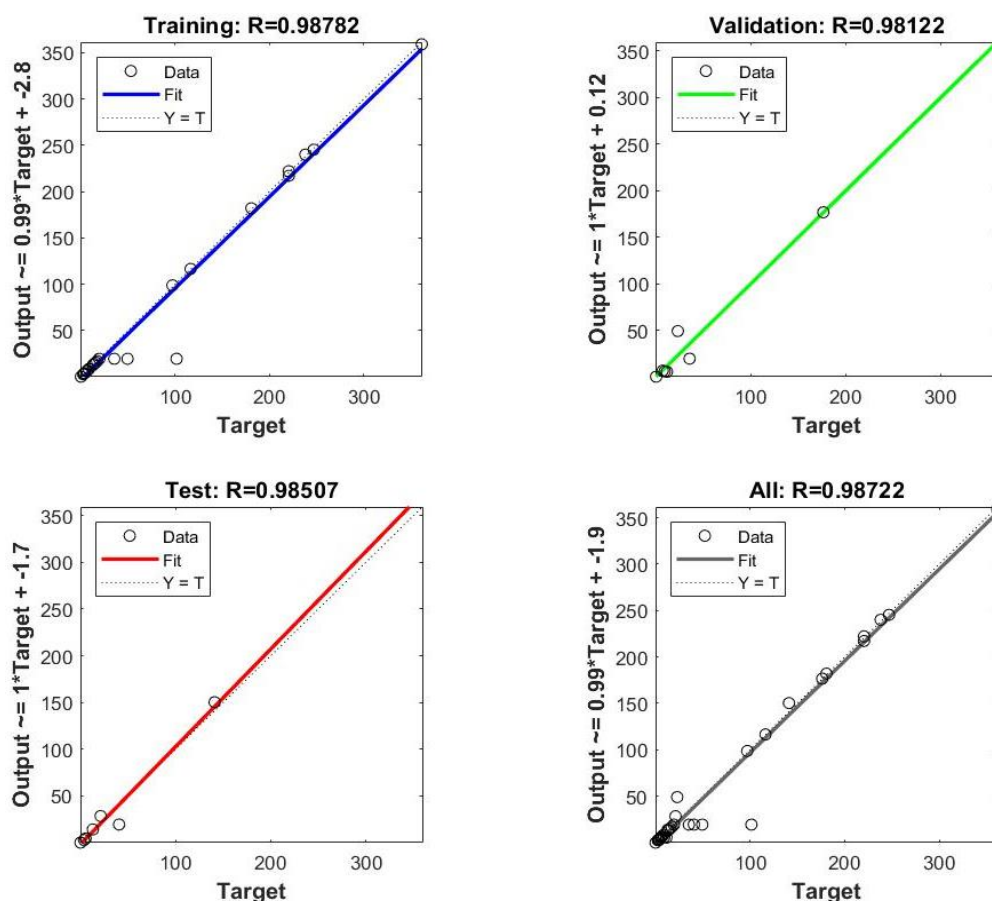


**Figure 7.** Artificial neural network (ANN) regression plot depicting results during training, validation, testing, and combined percentage.

Figure 7 shows the network's formulation of the overall R value: MRR, Oc and TW results are also significantly correlated with the ANN predicted values described in Equation (8) to Equation (11):

$$Output = 0.99 * Target - 2.8 \text{ for training} \quad (8)$$

$$\text{Output} = 1 * \text{Target} + 0.12 \text{ for validation} \quad (9)$$

$$\text{Output} = 1 * \text{Target} - 1.7 \text{ for testing} \quad (10)$$

$$\text{Output} = 0.99 * \text{Target} - 1.9 \text{ for combined} \quad (11)$$

Zn/(Ag + Fe)-MMC micro-drilling parameters were successfully modeled using ANNs. It is observed from Figures 8, 9, and 10. Validation of ANN models for MRR, Oc, and TW results in close prediction as similar to experimental observations. Figures 8 to 10 show the validation for the MRR, Oc, and TW values, respectively, using ANN. Figures 8–10 show that the root mean square error between experimental and predicted values for MRR (minimum = 6.06E-06 and maximum = 19.32), Oc (minimum = 0.001268 and maximum = 1.22), and TW (minimum = 0.000165 and maximum = 0.0056) are all within acceptable limits. Testing all the training and testing patterns for MRR, Oc, and TW resulted in an average root mean square error of 2.36%, 1.38%, and 0.13% respectively. MRR, Oc, and TW have all been predicted satisfactorily by the ANN model.

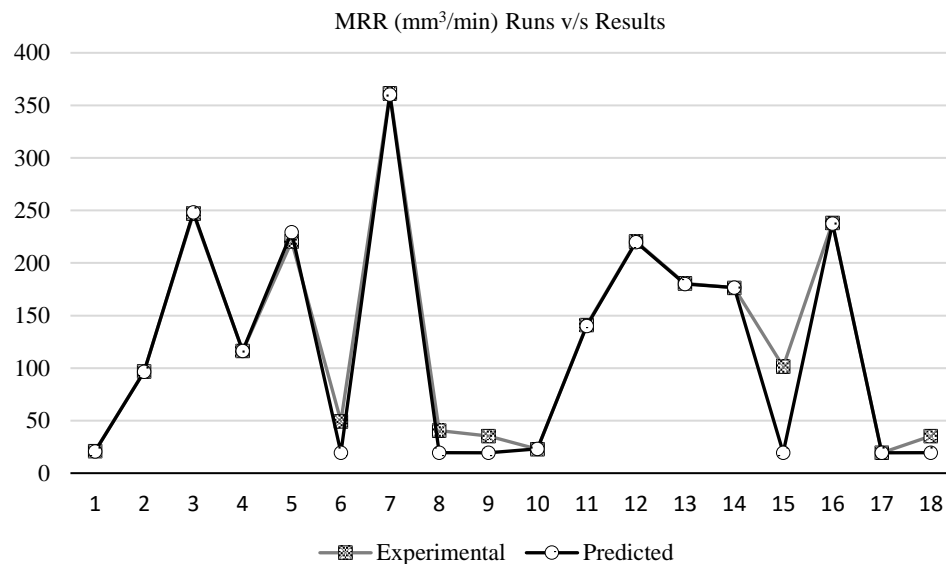


**Figure 8.** Validation of artificial neural network (ANN) model for material removal rate (MRR).

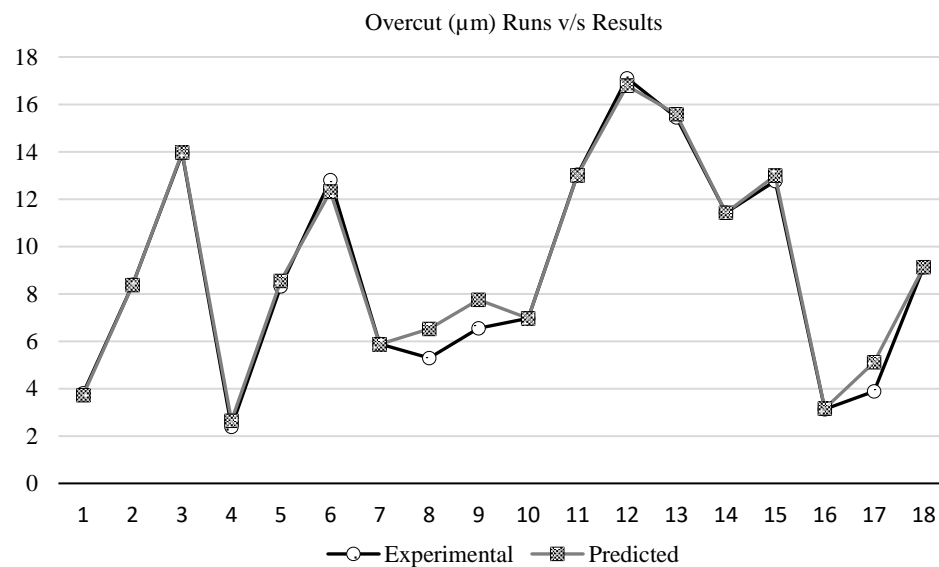


**Figure 9.** Validation of artificial neural network (ANN) model for overcut (Oc).

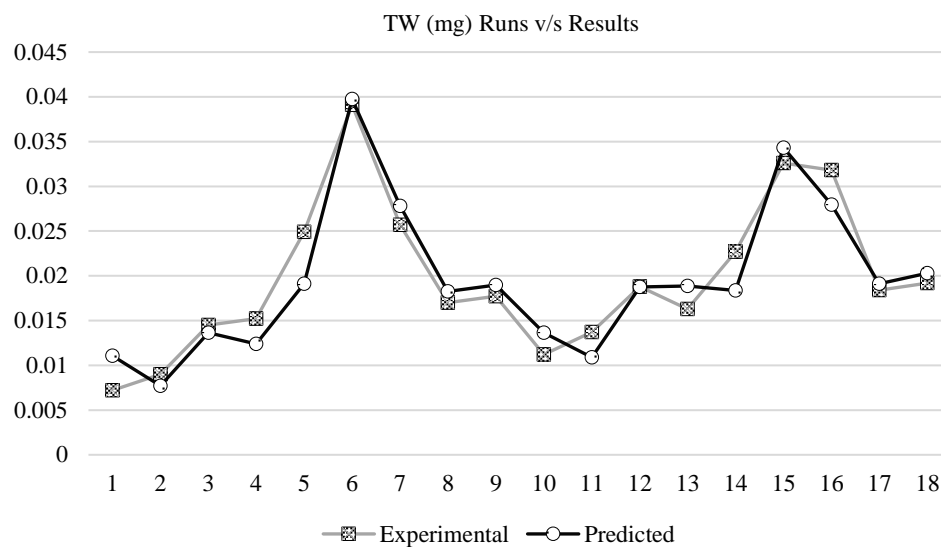


**Figure 10.** Validation of artificial neural network (ANN) model for tool wear (TW).

### INTERPRETATION, CONCLUSION AND LIMITATION

Brass micro-drills were used for ECDM experiments to collect MRR,  $O_c$ , and TW data under different drilling conditions involving pulse-on-time, pulse-off-time, current, and feed rate combinations. Testing was conducted to obtain optimal material removal rate (maximum), tool wear (minimum), and overcut (minimum) in the least amount of time.

An ANN approach provides an effective and systematic method for optimization. Data have been learned using the ANN. A total of 18 patterns were used to train the four network configurations (4-16-3-3). Micro-drilled surfaces with fewer defects can be made possible with the use of tools for predicting and controlling the micro-drilling properties of fabricated novel Zn/(Ag+Fe)-MMC. Output of model and experimental results of MRR,  $O_c$ , and TW are closely matched, demonstrating the validity of neural network models. Additional predictions for non-experimental patterns are possible with this method, replacing existing regression analysis.

Whereas, experimenting with more dataset leads to more training data and can lead to higher accuracy. Authors used limited machining data due to constraint of fabricated zinc-based MMC and focused just to demonstrate ANN feasibility. With a regression value above 98.5%, there is also a strong agreement between the predicted and expected values of all three output functions, which shows the utility of ANNs for optimization problems. The ANN methodology is faster and more accurate than traditional methods.

### REFERENCES

1. Dubey AK, Yadava V. Laser beam machining—a review. *Int J Machine Tools Manuf.* 2008; 48: 609–628.
2. Notton G, Voyant C, Fouilloy A, Duchaud JL, Nivet MN. Some applications of ANN to solar radiation estimation and forecasting for energy applications. *Appl Sci.* 2019; 9 (1): 209.
3. Hassoun MH. *Fundamentals of Artificial Neural Networks.* Cambridge, MA: MIT Press; 1995.
4. Gupta N. Artificial neural network. *Netw Complex Syst.* 2013; 3: 24–28.
5. Haykin S. *Kalman Filtering and Neural Networks.* New York: John Wiley & Sons; 2004.
6. Kechagias JD, Ninikas K, Petousis M, Vidakis N, Vaxevanidis N. An investigation of surface quality characteristics of 3D printed PLA plates cut by CO<sub>2</sub> laser using experimental design. *Mater Manuf Process.* 2021; 36 (13): 1544–1553.
7. Tamrin K, Nukman Y, Sheikh N. Laser spot welding of thermoplastic and ceramic: an experimental investigation. *Mater Manuf Process.* 2015; 30: 1138–1145.

8. Manikandan N, Raju R, Palanisamy D, Binoj J. Optimisation of spark erosion machining process parameters using hybrid grey relational analysis and artificial neural network model. *Int J Machining Machinabil Mater.* 2020; 22: 1–23.
9. Kechagias J, Tsiolikas A, Asteris P, Vaxevanidis N. Optimizing ANN performance using DOE: application on turning of a titanium alloy. *MATEC Web of Conferences.* 2018; 178: Article 01017.
10. Vidakis N, Petousis M, Vaxevanidis N, Kechagias J. Surface roughness investigation of poly-jet 3D printing. *Mathematics.* 2020; 8 (10): 1758.
11. Tsiolikas A, Tsiamitros D, Kitsakis K, Kechagias J, Mastorakis N, Kaminaris SD. Optimization of neural network parameters using Taguchi robust design: application in plasma arc cutting process. In: 2017 Fourth International Conference on Mathematics and Computers in Sciences and in Industry (MCSI), IEEE, Corfu, Greece. 2017, August 24–27. pp. 57–61.
12. Janković P, Madić M, Radovanović M, Petković D, Mladenović S. Optimization of surface roughness from different aspects in high-power CO<sub>2</sub> laser cutting of AA5754 aluminum alloy. *Arab J Sci Eng.* 2019; 44: 10245–10256.
13. Albugami N, Avrutin E. Dynamic modelling of electrooptically modulated vertical compound cavity surface emitting semiconductor lasers. *Optic Quantum Electron.* 2017; 49: Article 307.
14. Yousef BF, Knopf GK, Bordatchev EV, Nikumb SK. Neural network modeling and analysis of the material removal process during laser machining. *Int J Adv Manuf Technol.* 2003; 22: 41–53.
15. Fotovvati B, Balasubramanian M, Asadi E. Modeling and optimization approaches of laser-based powder-bed fusion process for Ti-6Al-4V alloy. *Coatings.* 2020; 10: 1104.
16. McDonnell MD, Arnaldo D, Pelletier E, Grant-Jacob JA, Praeger M, Karnakis D, Eason RW, Mills B. Machine learning for multi-dimensional optimisation and predictive visualisation of laser machining. *J Intell Manuf.* 2021; 32: 1471–1483.
17. Mills B, Grant-Jacob JA. Lasers that learn: the interface of laser machining and machine learning. *IET Optoelectron.* 2021; 15 (5): 207–224.
18. Zhang Q, Wang Z, Wang B, Ohsawa Y, Hayashi T. Feature extraction of laser machining data by using deep multi-task learning. *Information.* 2020; 11: 378.
19. Madić MJ, Radovanović MR. Optimal selection of ANN training and architectural parameters using Taguchi method: a case study. *FME Trans.* 2011; 39: 79–86.
20. Kumar D, Gupta AK, Chandna P, Pal M. Optimization of neural network parameters using Grey–Taguchi methodology for manufacturing process applications. *Proc Inst Mech Eng Part C: J Mech Eng Sci.* 2015; 229: 2651–2664.
21. Zhou P, Erning JW, Ogle K. Interactions between elemental components during the dealloying of Cu-Zn alloys. *Electrochim Acta.* 2019; 293: 290–298.
22. Kecman V. *Learning and Soft Computing.* Cambridge, MA: MIT Press; 2000.
23. Das S, Bandyopadhyay PP, Chattopadhyay AB. Neural networks-based tool wear monitoring in turning medium carbon steel using a coated carbide tool. *J Mater Process Technol.* 1997; 63: 187–192.